MANTECH Publications

Journal of Research in Physics and Applied Sciences

Volume 4, Issue 1, January-June 2021

Spectral and Thermal Properties of Nd^{3+} Doped Zinc Lithium Antimony Soda lime Tantalum Tellurite Glasses

Dr. S. L. Meena

Assistant Professor

Department of Physics

Jai Narain Vyas University, Jodhpur 342001(Raj.) India

Corresponding Author's Email id: *shankardiya7@rediffmail.com*

Abstract

Glass of the system: (35-x) TeO_2:10ZnO:10Li_2O:10Sb_2O_3:10Na_2O:10CaO: 15Ta_2O_5:xNd_2O_3. (where x=1, 1.5,2 mol %) have been prepared by the melt-quenching method. The amorphous nature of the glasses was confirmed by X-ray diffraction studies. Optical absorption spectra were recorded at room temperature for all glass samples. Slater-Condon parameters F_k (k=2, 4, 6), Lande's parameter ξ_{4f} and Racah parameters E^k (k=1, 2, 3) have been computed. Using these parameters, energies and intensities of these bands have been calculated. Judd-Ofelt intensity parameters Ω_λ (λ=2, 4, 6) are evaluated from the intensities of various absorption bands of optical absorption spectra. Using these intensity parameters, various radiative properties like spontaneous emission probability (A), branching ratio (β_R), radiative lifetime (τ_R) and stimulated emission cross-section (σ_p)) of various emission lines have been evaluated.

Keywords*: - ZLASLTT Glasses, Optical Properties, Judd-Ofelt Theory, Rare earth ions.*

INTRODUCTION

Rare-earth ions doped in different glass hosts to achieve favourable potential applications in a variety of optical devices such as lasers, fiber amplifiers, optical, linear and non-linear properties [1-5]. Among different glass matrices, scientific interest in tellurite glasses is attributed to their favorable properties such as high refractive index, high density, large third-

Page 9-20 © MANTECH PUBLICATIONS 2021. All Rights Reserved

order non-linear optical susceptibility [6-9]. Tellurite glass is an extremely promising material for laser and non-linear applications in optics due to some of its essential characteristic features, such as low phonon maxima, low melting temperature and excellent transparency in the far-infrared region [10-12]. The optical properties of rare-earth ions in glasses vary in a wide range that depends on the chemical composition of glass former and glass modifier. The addition of Na_2O to the glass mixture improves the rare earth ion solubility leading to the possibility of using even higher concentrations of ions. TeO_2 is known as a conditional glass former; it needs a modifier ion to form the glassy state easily. The addition of network modifier (NWF) Li_2O is to improve both the electrical and mechanical properties of such glasses. Zinc oxide is added to the glass matrix to increase glass-forming ability and to ensure low rates of crystallization in the glass system [13-18].

The present work reports on the absorption and emission properties of Nd^{3+} doped zinc lithium antimony soda lime tantalum tellurite glasses. The intensities of the transitions for the rare earth ions have been estimated successfully using the Judd-Ofelt theory; the laser parameters such as radiative probabilities (A), branching ratio (β_R), radiative lifetime (τ_R) and stimulated emission cross-section(σ_p) are evaluated using J.O. intensity parameters (Ω_λ, λ=2,4 and 6).

EXPERIMENTAL TECHNIQUES

Preparation of Glasses

The following Nd^{3+} doped zinc lithium antimony soda-lime tantalum tellurite Glasses glass samples (35-x) TeO_2:10ZnO: 10Li_2O:10Sb_2O_3:10Na_2O:10CaO:15Ta_2O_5: xNd_2O_3. (where *x* =1, 1.5, 2) have been prepared by the melt-quenching method. Analytical reagent grade chemicals used in the present study consist of TeO_2, ZnO, Li_2O, Sb_2O_3, Na_2O, CaO, Ta_2O_5 and Nd_2O_3. They were thoroughly mixed by using an agate pestle mortar and then melted at 1060˚C by an electrical muffle furnace for 2 hours. After complete melting, the melts were quickly poured into a preheated stainless steel mould and annealed at a temperature of 350˚C for 2 h to remove thermal strains and stresses. Every time the fine powder of cerium oxide was used for polishing the samples. The glass samples so prepared were of good optical quality and were transparent. The chemical compositions of the glasses with the name of samples are summarized in **Table 1.**

Page 9-20 © MANTECH PUBLICATIONS 2021. All Rights Reserved

Table 1

Sample	Glass composition (mol %)
ZLASLTT (UD)	$35TeO_2$:10ZnO:$10Li_2O$:$10Sb_2O_3$:10 Na_2O:10CaO:$15Ta_2O_5$
ZLASLTT (ND1)	$34TeO_2$:10ZnO:$10Li_2O$:$10Sb_2O_3$:$10Na_2O$:10CaO:$15Ta_2O_5$:$1Nd_2O_3$
ZLASLTT (ND1.5)	$33.5TeO_2$:10ZnO:$10Li_2O$:$10Sb_2O_3$:10 Na_2O:10CaO:$15Ta_2O_5$:$1.5Nd_2O_3$
ZLASLTT (ND2)	$33TeO_2$:10ZnO:$10Li_2O$:$10Sb_2O_3$:$10Na_2O$:10CaO:$15Ta_2O_5$: $2Nd_2O_3$

ZLASLTT (UD)-Represents undoped zinc lithium antimony soda-lime tantalum tellurite glass specimens.

ZLASLTT (ND)-Represents Nd^{3+} doped zinc lithium antimony soda-lime tantalum tellurite glass specimens.

THEORY

1. *Oscillator Strength*

The intensity of spectral lines is expressed in terms of oscillator strengths using the relation [19].

$$f_{expt.} = 4.318 \times 10^{-9} \int \varepsilon(\nu)\, d\nu \qquad (1)$$

Where, $\varepsilon(\nu)$ is the molar absorption coefficient at a given energy ν (cm^{-1}), to be evaluated from Beer-Lambert law.

Under Gaussian Approximation, using Beer-Lambert law, the observed oscillator strengths of the absorption bands have been experimentally calculated [20], using the modified relation:

$$P_m = 4.6 \times 10^{-9} \times \frac{1}{cl} \log \frac{I_0}{I} \times \Delta\upsilon_{1/2} \qquad (2)$$

Where, c is the molar concentration of the absorbing ion per unit volume, I is the optical path length, $\log I_0/I$ is optical density and $\Delta\upsilon_{1/2}$ is half bandwidth.

2. *Judd-Ofelt Intensity Parameters*

According to Judd [21] and Ofelt [22] theory, independently derived an expression for the oscillator strength of the induced forced electric dipole transitions between an initial J manifold $|4f^N (S, L) J\rangle$ level and the terminal J' manifold $|4f^N (S', L') J'\rangle$ is given by:

Page 9-20 © MANTECH PUBLICATIONS 2021. All Rights Reserved

$$\frac{8\Pi^2 mc\,\upsilon}{3h\,(2J+1)}\left[\frac{(n^2+2)^2}{9}\right]\times S(J,J') \quad (3)$$

Where, the line strength S (J, J') is given by the equation.

$$S(J,J') = e^2 \sum \Omega_\lambda \langle 4f^N(S,L)\,J \| U^{(\lambda)} \| 4f^N(S',L')\,J' \rangle^2 \quad (4)$$

$\lambda = 2, 4, 6$

In the above equation, m is the mass of an electron, c is the velocity of light, v is the wave number of the transition, h is Planck's constant, n is the refractive index, J and J' are the total angular momentum of the initial and final level respectively, Ω_λ (λ=2,4and 6) are known as Judd-Ofelt intensity parameters.

3. *Radiative Properties*

The Ω_λ parameters obtained using the spectral absorption results have been used to predict radiative properties such as spontaneous emission probability (A) and radiative lifetime (τ_R), and laser parameters like fluorescence branching ratio (β_R) and stimulated emission cross-section (σ_p).

The spontaneous emission probability from initial manifold $|4f^N\,(S',\,L')\,J'\rangle$ to a final manifold $|4f^N\,(S,L)\,J\rangle$ is given by:

$$A[(S',L')J';(S,L)J] = \frac{64\pi^4\nu^3}{3h(2J'+1)}\left[\frac{n(n^2+2)^2}{9}\right]\times S(J',J) \quad (5)$$

Where, $S(J',J) = [\Omega_2 \| U^{(2)} \|^2 + \Omega_4 \| U^{(4)} \|^2 + \Omega_6 \| U^{(6)} \|^2]$

The fluorescence branching ratio for the transitions originating from a specific initial manifold $|4f^N\,(S',\,L')\,J'\rangle$ to a final many fold $|4f^N\,(S,L)J\rangle$ is given by

$$\beta[(S',L')J';(S,L)J] = \sum_{S\,L\,J}\frac{A[(S'\,L')]}{A[(S'\,L')\,J'(\bar{S}\,L)]} \quad (6)$$

The radiative lifetime is given by

$$\tau_{rad} = \sum_{S\,L\,J} A[(S',L')J';(S,L)] = A^{-1}_{Total} \quad (7)$$

Page 9-20 © MANTECH PUBLICATIONS 2021. All Rights Reserved

Where, the sum is over all possible terminal manifolds. The stimulated emission cross-section for a transition from an initial manifold $|4f^N (S', L') J'>$ to a final manifold $|4f^N (S, L)J >|$ is expressed as

$$\sigma_p(\lambda_p) = [\frac{\lambda_p^4}{8\pi c n^2 \Delta\lambda_{eFF}}] \times A[(S', L')J'; (S, L)J] \quad (8)$$

Where, λ_p the peak fluorescence wavelength of the emission band and $\Delta\lambda_{eff}$ is the effective fluorescence line width.

RESULT AND DISCUSSION

1. *XRD Measurement*

Figure 1 presents the XRD pattern of the samples, shows no sharp Bragg's peak but only a broad diffuse hump around the low angle region. This is a clear indication of the amorphous nature within the resolution limit of the XRD instrument.

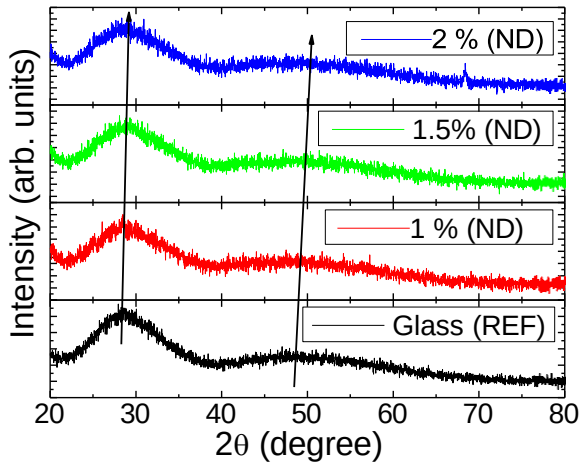


Fig. 1: X-ray diffraction pattern of TeO_2:ZnO:Li_2O:Sb_2O_3:Na_2O:CaO:Nd_2O_3 glasses

2. *Thermal Property*

Figure 2 shows the thermal properties of ZLASLTT glass from 300^0C to 1000^0C. From the DSC curve of the present glasses system, I can find out that no crystallization peak is apparent and the glass transition temperature T_g are 352,450 and 582, respectively. The T_g increase with the contents of Nd_2O_3 increase. I could conclude that the thermal properties of the ZLASLTT glass are good for fiber drawing from the analysis of the DSC curve.

Page 9-20 © MANTECH PUBLICATIONS 2021. All Rights Reserved

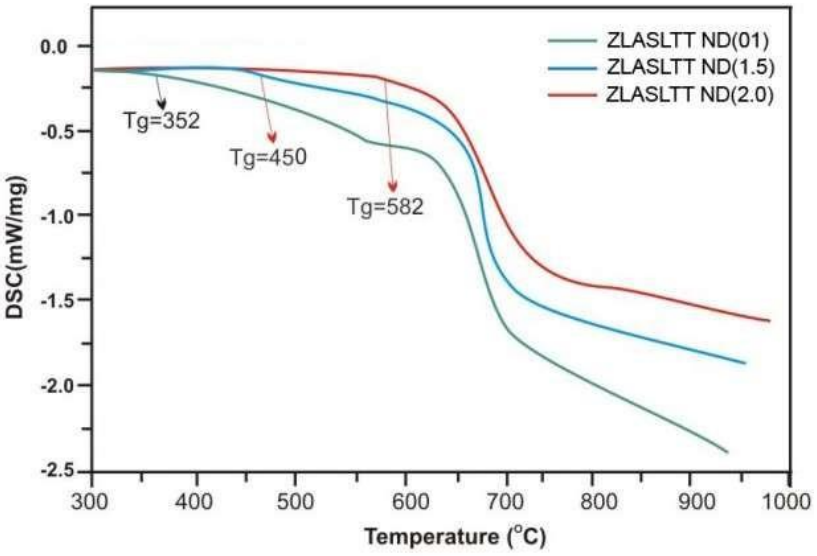


Fig. 2: DSC curve of ZLASLTT (ND) glasses.

3. *Absorption Spectra*

The absorption spectra of ZLASLTT (ND01) glass consists of absorption bands corresponding to the absorptions from the ground state $^4I_{9/2}$ of Nd^{3+} ions. Nine absorption bands have been observed from the ground state $^4I_{9/2}$ to excited states $^4F_{3/2}$, $^4F_{5/2}$, $^4F_{7/2}$, $^4F_{9/2}$, $^2H_{11/2}$, $^4G_{5/2}$, $^4G_{7/2}$, $^4G_{9/2}$, and $^2G_{9/2}$ for Nd^{3+} doped ZLASLTT(ND 01) glass.

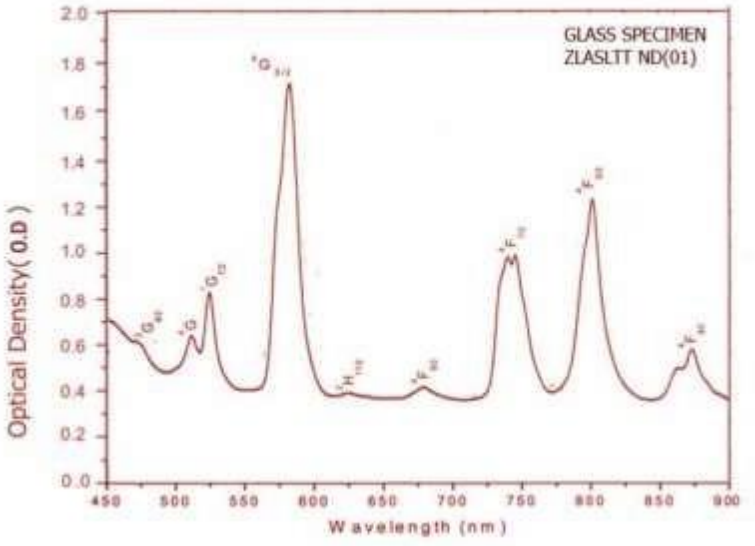


Fig. 3: Absorption spectra of ZLASLTT (ND 01) glass.

The experimental and calculated oscillator strength for Nd3+ ions in ZLASLTT glasses is given in **Table 2.**

Page 9-20 © MANTECH PUBLICATIONS 2021. All Rights Reserved

Table 2: Measured and calculated oscillator strength ($P^m \times 10^{+6}$) of Nd^{3+} ions in ZLASLTT glasses.

Energy level from $^4I_{9/2}$	**Glass ZLASLTT (ND01)**		**Glass ZLASLTT (ND1.5)**		**Glass ZLASLTT (ND02)**	
	$P_{exp.}$	**$P_{cal.}$**	**$P_{exp.}$**	**$P_{cal.}$**	**$P_{exp.}$**	
$^4F_{3/2}$	4.36	4.38	3.64	3.74	2.95	
$^4F_{5/2}$	9.54	9.41	8.55	8.42	7.65	
$^4F_{7/2}$	9,73	10.18	8.88	9.40	7.84	8.41
$^4F_{9/2}$	0.79	0.564	0.635	0.513	0.588	0.454
$^2H_{11/2}$	0.44	0.162	0.372	0.146	0.279	0.129
$^4G_{5/2}$	25.68	25.99	24.78	25.14	23.82	24.16
$^4G_{7/2}$	4.83	5.82	3.95	5.21	3.23	4.63
$^4G_{9/2}$	2.67	2.61	2.14	2.28	1.96	1.97
$^2G_{9/2}$	0.97	3.40	0.86	2.94	0.78	2.50
R.m.s.deviation	0.9041		0.8434		0.7833	

Computed values of Slater-Condon, Lande', Racah, nephelauxetic ratio and bonding parameter for Nd^{3+} doped ZLASLTT glass specimens are given in **Table 3**.

Table 3: Computed values of Slater-Condon, Lande', Racah, nephelauxetic ratio and bonding parameter for Nd^{3+} doped ZLASLTT glass specimens.

Parameter	**Free ion**	**ZLASLTT(ND01)**	**ZLASLTT(ND1.5)**	**ZLASLTT (ND02)**
$F_2(cm^{-1})$	331.16	324.62	324.59	324.60
$F_4(cm^{-1})$	50.71	50.70	50.72	550.730
$F_6(cm^{-1})$	5.154	5.070	5.039	5.040
$\xi_{4f}(cm^{-1})$	884.0	882.97	882.78	882.57
$E^1(cm^{-1})$	5024.0	4947.38	4947.22	4947.83
$E^2(cm^{-1})$	23.90	23.089	23.079	23.077
$E^3(cm^{-1})$	497.0	489.56	489.57	489.59
F_4/F_2	0.1531	0.1562	0.1562	0.1553
F_6/F_2	0.0155	0.01553	0.015524	0.015526
E^1/E^3	10.1086	10.1058	10.1052	10.1061
E^2/E^3	0.0481	0.047162	0.04714	0.04713
β'		0.99584	0.99582	0.99598
$b^{1/2}$		0.04561	0.04571	0.044840

Page 9-20 © MANTECH PUBLICATIONS 2021. All Rights Reserved

Judd-Ofelt intensity parameters Ω_λ (λ = 2, 4 and 6) were calculated by using the fitting approximation of the experimental oscillator strengths to the calculated oscillator strengths with respect to their electric dipole contributions.

The values of Judd-Ofelt intensity parameters are given in **Table 4**.

Table 4: Judd-Ofelt intensity parameters for Nd^{3+} doped ZLASLTT glass specimens

Glass Specimen	Ω_2(pm^2)	Ω_4(pm^2)	Ω_6(pm^2)	Ω_4/Ω_6	Ref.
ZLASLTT(ND01)	1.298	8.570	3.232	2.652	P.W.
ZLASLTT (ND1.5)	2.028	7.251	3.031	2.392	P.W.
ZLASLTT (ND02)	2.623	6.073	2.743	2.214	P.W.
PMMA(ND)	2.11	3.78	2.61	1.448	[23]
Fluorophosphate(ND)	1.83	4.73	4.19	1.129	[24]

4. *Fluorescence Spectrum*

The fluorescence spectrum of Nd^{3+}doped in zinc lithium antimony soda-lime tantalum tellurite glass is shown in **Figure 4.** There are three broad bands ($^4F_{3/2}\rightarrow{}^4I_{9/2}$) and ($^4F_{3/2}\rightarrow{}^4I_{11/2}$) and ($^4F_{3/2}\rightarrow{}^4I_{13/2}$) respectively for glass specimens.

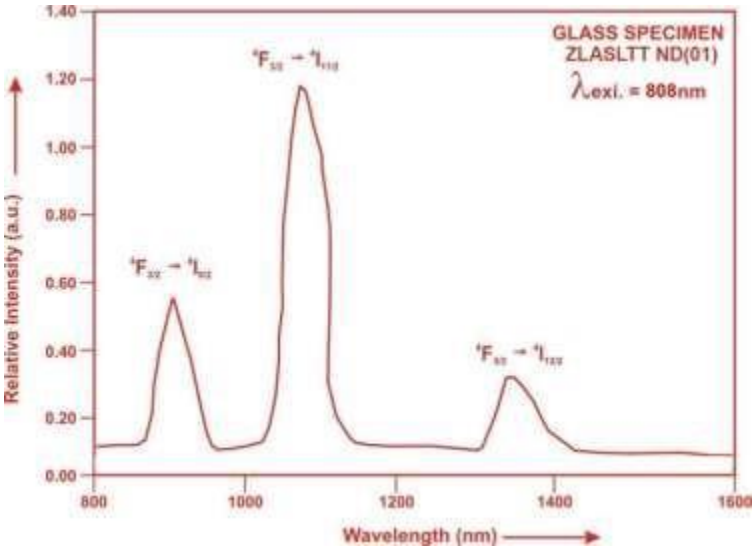


Fig. 4: Fluorescence spectrum of ZLASLTT glasses doped with Nd^{3+}

The wavelengths of these bands, along with their assignments, are given in **Table 5**.

Page 9-20 © MANTECH PUBLICATIONS 2021. All Rights Reserved

Table 5: Emission peak wave lengths (λ_p), radiative transition probability (A_{rad}), branching ratio (β_R), stimulated emission crosssection (σ_p), and radiative life time (τ_R) for various transitions in Nd^{3+} doped ZLASLTT glasses.

Transition		ZLASLTT (ND01)				ZLASLTT (ND01)				ZLASLTT (ND01)			
	λ_{max} (nm)	$A_{rad}(s^{-1})$	β	σ_p (10^{-20} cm^2)	τ_R(μs)	$A_{rad}(s^{-1})$	β	σ_p (10^{-20} cm^2)	τ_R (μs)	$A_{rad}(s^{-1})$	β	$\sigma_p(10^{-20}$ $cm^2)$	$\tau_R(10^{-20}$ $cm^2)$
$^4F_{3/2}\rightarrow{}^4I_{9/2}$	905	1073.42	0.6181	0.947	575.84	918.48	0.6060	0.832	659.84	776.43	0.5966	0.723	768.43
$^4F_{3/2}\rightarrow{}^4I_{11/2}$	1075	576.97	0.3322	2.853		516.03	0.3405	2.766		451.49	0.3469	2.727	
$^4F_{3/2}\rightarrow{}^4I_{13/2}$	1320	86.20	0.0496	0.450		81.02	0.0535	0.441		73.45	0.0564	0.421	

CONCLUSION

In the present study, the glass samples of composition (35-x) TeO2:10ZnO: $10Li_2O$:$10Sb_2O_3$:$10Na_2O$:10CaO:$15Ta_2O_5$: xNd_2O_3. (where x=1, 1.5, 2 mol %) have been prepared by the melt-quenching method. The value of stimulated emission cross-section (σ_p) is found to be maximum for the transition ($^4F_{3/2}\rightarrow{}^4I_{11/2}$) for glass ZLASLTT (ND 01), suggesting that glass ZLASLTT (ND 01) is better compared to the other two glass systems ZLASLTT (ND1.5) and ZLASLTT (ND02). The large stimulated emission cross-section for the transition ($^4F_{3/2}\rightarrow{}^4I_{11/2}$) for all glass specimens. This shows that ($^4F_{3/2}\rightarrow{}^4I_{11/2}$) transition is the most probable transition.

REFERENCES

I. Reddy, M.B., Sailaja, S., Girihar, P., Raju, C.N. and Reddy, B.S. (2011). Spectroscopic investigations of Sm^{3+} ions doped B_2O_3-Bi_2O_3-ZnO-Li_2O glasses, Ferroelectric letters 38, 50.

II. Chen, R., Tian, Y., Li, B., Wang, F., Jing, X. and Zhang, J. (2015). 2 μm fluorescence of Ho^{3+}:$^5I_7\rightarrow{}^5I_8$ transitions sensitized by Er^{3+} in telluritegermanate glasses, Opt. Mater.49, 116–122.

III. Zhao, J., Zheng, X., Schartner, E.P., Ionescu, P., Zhang, R., Nguyen, T.-L., Jin, D. and Ebendorff- Heidepriem, H.(2016).

Page 9-20 © MANTECH PUBLICATIONS 2021. All Rights Reserved

Up conversion nanocrystal-doped glass: A new paradigm for photonic materials. Adv. Opt. Mater. 4, 1507.

IV. Serqueira, E.O., Dantas, N.O., Bell, M.J.V. (2011).Control of spectroscopic fluorescence parameters of Nd^{3+} ions as a function of concentration in a SiO_2–Na_2O–Al_2O_3–B_2O_3 glass system. Chem. Phys. Lett. 508, 125–129.

V. Xu, Y., Li, S., Hu, L., Chen, W. (2011).Effect of copper impurity on the optical loss and Nd^{3+}nonradiative energy loss of Nd-doped phosphate laser glass. J. Rare Earths 29, 614–617.

VI. Flórez, A., Martı´nez, J.F., Flórez, M., Porcher, P. (2001).Optical transition probabilities and compositional dependence of Judd–Ofelt parameters of Nd^{3+} ions influoroindate glasses. J. Non-Cryst. Solids 284, 261–267.

VII. Anjaiah, J. and Laxmikanth, C. (2015).Optical Properties of Neodymium Ion Doped Lithium Borate Glasses, 5,173.

VIII. Peng, M. and Wondraczek, L. (2009).Bismuth-Doped Oxide Glasses as Potential Solar Spectral Converters and Concentrators, J. Mater. Chem., 19, 627.

IX. Durga, D.K.; Veeraiah, N. (2003). Role of manganese ions on the stability of ZnF_2–P_2O_5–TeO_2 glass system by the study of dielectric dispersion and some other physical properties. J. Phys. Chem. Solids, 64, 133–146.

X. Wang, J.S., Vogel, E.M., Snitzer, E., (1994). Tellurite glass: a new candidate for fiber devices. Opt. Mater. 3, 187–203.

XI. Malik M. S. and Hogarth, C. A.(1989).“Some optical properties of TeO_2-CuO-Lu_2O_3 glasses,” Journal of Materials Science Letters, vol. 8, no. 6, pp. 655–659, 1989.

XII. Babu, A.M., Jamalaiah, B.C., Kumar, J.S., Sasikala, T. and Moorthy, L.R. (2011). Spectroscopic and photoluminescence properties of Dy^{3+}-doped lead tungsten tellurite glasses for laser materials, Journal

Page 9-20 © MANTECH PUBLICATIONS 2021. All Rights Reserved

of Alloys and Compounds 509, 457-462.

XIII. Pavani, P. G., Sadhana, K. and Mouli, V. C. (2011). "Optical, physical and structural studies of boro-zinc tellurite glasses," Physica B: Condensed Matter, vol. 406, no. 6-7, pp. 1242–1247.

XIV. Rao, T.V.R., Reddy, R.R., Nazeer Ahammed, Y., Parandamaiah, M. (2000). Luminescence properties of Nd^{3+}, TeO_2-B2O3–P2O5–Li2O glass. Infrared Physics & Technology, 41: 247.

XV. Upender, G., Sathe, V.G. and Mouli, V.C. (2009).Raman spectroscopic characterization of tellurite glasses containing heavy metal oxides, Phys. B Phys. Condens. Matter. 405, 1269–1273.

XVI. Stambouli, W., Elhouichet, H., Gelloz, B., Feid, M.(2013).Optical and spectroscopic properties of Eu-doped tellurite glasses and glass ceramics, 138, 201–208.

XVII. Upendra, K. K., Prathyusha, V.A., Babu, P., Jayasankar, C.K., Joshi, A.S., Speghini, A. and Bettinelli, M. (2007). Fluorescence properties of Nd^{3+}-doped tellurite glasses, Spectrochimica Acta Part A, 67: 702.

XVIII. Venkateswarlu ,M., Mahamuda, S.K., Swapna, K., Prasad, M.V.V.K.S., Rao, A. S., Babu, A. M., Shakya ,S., Vijaya Prakash ,G. (2015) .Spectroscopic studies of Nd^{3+}doped lead tungsten tellurite glasses for the NIR emission at 1062 nm, Optical Materials39,815.

XIX. Gorller-Walrand, C. and Binnemans, K. (1988). Spectral Intensities of f-f Transition. In: Gshneidner Jr., K.A. and Eyring, L., Eds., Handbook on the Physics and Chemistry of Rare Earths, Vol. 25, Chap. 167, North-Holland, Amsterdam, 101-264.

XX. Sharma, Y.K., Surana, S.S.L. and Singh, R.K. (2009). Spectroscopic Investigations and Luminescence Spectra of Sm^{3+} Doped Soda Lime Silicate Glasses. Journal of Rare Earths, 27, 773.

XXI. Judd, B.R. (1962). Optical Absorption Intensities of Rare

Page 9-20 © MANTECH PUBLICATIONS 2021. All Rights Reserved

Earth Ions. Physical Review, 127, 750.

XXII. Ofelt, G.S. (1962). Intensities of Crystal Spectra of Rare Earth Ions. The Journal of Chemical Physics, 37, 511.

XXIII. Silva, M.C., Cristovan, F.H., Nascimento, C.M., Bell, M.J.V., Cruz, W.O., Marletta, A. (2006). Judd-Ofelt analysis of Nd^{3+} ions in poly (styrene sulfonate) films. J. Non-Cryst. Solids 352, 5296–5300.

XXIV. Choi, J.H., Margaryan, A., Shi, F.G. (2005). Judd-Ofelt analysis of spectroscopic properties of Nd^{3+}-doped novel fluorophosphates glass. J. Lumin. 114, 167–177.

Page 9-20 © MANTECH PUBLICATIONS 2021. All Rights Reserved